Observing the superposition of a single particle with the vacuum

L. M. Rico Gutiérrez, V. Palge, and J. A. Dunningham
School of Physics and Astronomy, University of Leeds, Leeds LS2 9JT, United Kingdom

A defining feature of quantum mechanics is that it allows systems to exist in a superposition of different eigenstates of certain observables such as position or spin. Superpositions of other quantities such as mass or charge however are not seen in nature. It is thought that this disparity is partly due to the fact that it is much easier to carry out interference experiments for certain observables than others. Here we present an interferometry scheme that should allow us to observe interference between the vacuum and a single photon or atom. We begin by presenting a scheme for a Hadamard gate that operates in the Fock state basis and then show how, by creating an interferometer from two such gates, interference between a single particle and the vacuum could indeed be observed. This would provide evidence of a superposition of different particle numbers.

PACS numbers: 03.65.Ta 03.75.Dg

I. INTRODUCTION

An important part of quantum mechanics is the existence of superselection rules for certain quantities [1]. These are invoked to explain why, in practice, we do not observe certain superpositions such as states with different charge or mass. The need for these superselection rules, however, was challenged by Aharonov and Susskind [2] in the 1960s when they proposed a thought experiment to observe coherent superpositions of different charge states. Their work showed that it is important that there is an appropriate reference frame in order to observe the coherence [2–7]. For some quantities, reference frames are readily available: to observe coherences between different spin or polarisation states, for example, we only need a well-defined spatial axis as our reference. This means that such superpositions are commonly observed. But, for other quantities, the appropriate reference frames are much less obvious and so it is much harder to observe a superposition. Interestingly, this does not mean they cannot be observed so long as an appropriate reference frame can be found.

Other authors have extended the ideas of Aharonov and Susskind and applied them to different systems [3–5, 8]. Recent work, for example, has considered whether it might be possible to observe interference fringes that are due to a superposition of an atom and a molecule [6, 7], i.e. two states with different mass. Here we address the problem of whether we can observe superpositions of different Fock states for both atomic and optical systems. There has been a lot of interest lately in the related question of whether a single particle can be entangled and whether this entanglement can be used in quantum information schemes [9–15]. In this paper we consider the specific case of a superposition of a single particle (atom or photon) and the vacuum, i.e.

$$|\psi\rangle = \frac{1}{\sqrt{2}}\left(|0\rangle + |1\rangle\right), \tag{1}$$

and present the details of a specific interferometric scheme that could be used to observe this superposition.

We stress that state (1) is quite different from the one created by passing a single particle through a 50:50 beam splitter. A typical two-port beam splitter is a semi-reflective mirror that reflects part of the incident light and transmits the remainder. In general, this performs the following unitary transformation on the input state, $|\psi_{\rm in}\rangle$,

$$|\psi_{\rm out}\rangle = e^{iH_{BS}}|\psi_{\rm in}\rangle, \tag{2}$$

where H_{BS} is the interaction Hamiltonian for the beam splitter given by,

$$H_{BS} = \theta\left(e^{i\phi}a_{\rm in}^{\dagger}b_{\rm in} + e^{-i\phi}a_{\rm in}b_{\rm in}^{\dagger}\right). \tag{3}$$

The physical beam splitter can be described by any choice of θ and ϕ depending on the setup and fabrication, where θ is a measure of the transmittivity, and ϕ gives the phase shift due to the coating of the mirror [16]. In our case, we consider 50-50 beam splitters with $\theta = \pi/4$ and $\phi = 0$. Correspondingly, the incoming creation operators can be shown to be transformed in the following way

$$a_{\rm out}^{\dagger} = Ua_{\rm in}^{\dagger}U^{\dagger} = \cos\theta a_{\rm in}^{\dagger} + ie^{-i\phi}\sin\theta b_{\rm in}^{\dagger}, \tag{4}$$

$$b_{\rm out}^{\dagger} = ie^{i\phi}\sin\theta a_{\rm in}^{\dagger} + \cos\theta b_{\rm in}^{\dagger}, \tag{5}$$

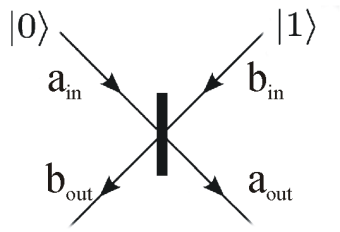

FIG. 1: Incoming and outgoing modes in a beam splitter.

and similar expressions for the annihilation operators. Thus, using Eqs.(4)-(5) we can easily calculate the transformation of any input to the beam splitter, for example

$$\begin{aligned} |1\rangle_a|0\rangle_b = a^\dagger_{\rm in}|0\rangle_a|0\rangle_b \longrightarrow a^\dagger_{\rm out}|0\rangle_a|0\rangle_b \quad &= \tfrac{1}{\sqrt{2}}\left(ib^\dagger_{\rm in} + a^\dagger_{\rm in}\right)|0\rangle_a|0\rangle_b \\ &= \tfrac{1}{\sqrt{2}}\left(i|0\rangle_a|1\rangle_b + |1\rangle_a|0\rangle_b\right) \\ &= \tfrac{1}{\sqrt{2}}\left(i|0\rangle_a|1\rangle_b + |1\rangle_a|0\rangle_b\right). \end{aligned} \tag{6}$$

Where the two modes a and b are the ones depicted in Figure 1. However, we will drop the subindices in the states and use the convention that the state that appears on the left of a product of states is associated with the left input or output of the beam splitter and a similarly for the right. Consequently, using this convention the transformation resulting in Eq.(6) reads

$$|1\rangle|0\rangle \longrightarrow \frac{1}{\sqrt{2}}\left(i|1\rangle|0\rangle + |0\rangle|1\rangle\right). \tag{7}$$

The most notable difference between this state and (1) is that the beam splitter conserves particle number whereas state (1) does not.

Superpositions of the form of (1) could be achieved by the action of a Hadamard gate (H) in the Fock basis $\{|0\rangle, |1\rangle\}$:

$$|0\rangle \xrightarrow{H} \frac{1}{\sqrt{2}}\left(|0\rangle + |1\rangle\right) \tag{8}$$

$$|1\rangle \xrightarrow{H} \frac{1}{\sqrt{2}}\left(|0\rangle - |1\rangle\right) \tag{9}$$

In fact, any unitary operation that transforms $|0\rangle$ and $|1\rangle$ into two orthogonal states that are each equally weighted superpositions of $|0\rangle$ and $|1\rangle$ will do. We could then observe the superposition by means of an interferometer. In other words, after the first Hadamard gate, we apply a phase shift, and then a second Hadamard. If the probability of detecting a particle or not at the output can be coherently controlled by adjusting the phase shift, that is a signature that a superposition of the form of (1) has been created. So the key element to our scheme is a Hadamard gate that operates in the basis $\{|0\rangle, |1\rangle\}$. Before we go on to discuss how this might be realised, we first introduce a technique that will form an important part of the scheme.

II. QUANTUM STATE TRUNCATION

Quantum state truncation (QST) was first put forward by Pegg and coworkers [17] and involves creating truncated versions of quantum superpositions conditioned on particular measurement outcomes. To take a particular example, suppose we had a coherent state with amplitude α and phase θ, i.e. $|\alpha e^{i\theta}\rangle_c$. This coherent state can be written as a superposition of Fock states,

$$|\alpha e^{i\theta}\rangle_c = e^{-|\alpha|^2/2}\sum_{n=0}^{\infty}\frac{(\alpha e^{i\theta})^n}{\sqrt{n!}}|n\rangle. \tag{10}$$

Throughout this paper, we will use a subscript c to denote coherent states; kets without a subscript are taken to be Fock states. Suppose, now, that we want to keep only the first two terms of the superposition, i.e. the ones

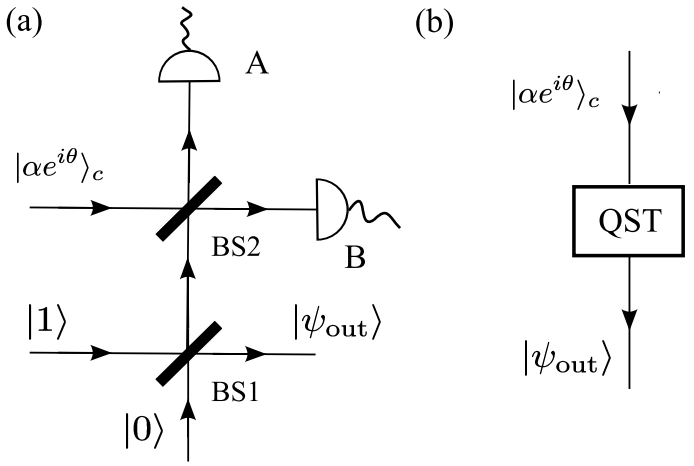

FIG. 2: Quantum state truncation scheme. (a) The Fock states $|0\rangle$ and $|1\rangle$ are fed into a 50:50 beam splitter (BS1) and one output is combined with the coherent state $|\alpha e^{i\theta}\rangle_c$ at a second 50:50 beam splitter (BS2). Depending on the measurement outcomes at detectors A and B, it is possible to achieve a truncated version of the coherent state at the output. For simplicity, the quantum state truncation scheme will be depicted as a 'black box' (as shown in (b)) in the remainder of the paper.

corresponding to $|0\rangle$ and $|1\rangle$. We can achieve this by using the QST scheme shown in Figure 2(a), which works as follows. We feed a single particle and a vacuum state respectively into the two inputs of a 50:50 beam splitter (BS1 in Figure 2(a)). One of the outputs is then combined with our coherent state at a second beam splitter (BS2). The outputs from BS2 are recorded at detectors A and B and if one particle is detected at A and none at B, then the remaining (and as yet unaccounted for) output from BS1 is the truncated state that we wanted, i.e.

$$|\psi_{\rm out}\rangle = \frac{1}{\sqrt{|\alpha|^2+1}}\left(|0\rangle + \alpha e^{i\theta}|1\rangle\right). \tag{11}$$

We can see this result by explicity calculating how the input state is transformed by the setup shown in Figure 2(a). The initial state is:

$$|\psi_{\rm in}\rangle = |\alpha e^{i\theta}\rangle_c|1\rangle|0\rangle = \left(|0\rangle + \alpha e^{i\theta}|1\rangle + \cdots\right)|1\rangle|0\rangle, \tag{12}$$

where we have expanded the coherent state in the Fock basis and ignored any overall normalisation. The last two kets (qubits) are then transformed by BS1 to give

$$\left(|0\rangle + \alpha e^{i\theta}|1\rangle + \cdots\right)\left(i|1\rangle|0\rangle_{\rm out} + |0\rangle|1\rangle_{\rm out}\right), \tag{13}$$

where the second qubit is directed towards BS2, and the last qubit is directed towards the output mode. Next, the first two qubits are transformed by BS2 to give the outputs at A and B. This gives,

$$\begin{aligned} & |0\rangle_A|0\rangle_B|1\rangle_{\rm out} \\ + \;& |0\rangle_A|1\rangle_B\left(-|0\rangle_{\rm out} + \alpha e^{i\theta}|1\rangle_{\rm out}\right) \\ + \;& i|1\rangle_A|0\rangle_B\left(|0\rangle_{\rm out} + \alpha e^{i\theta}|1\rangle_{\rm out}\right) \\ + \;& \cdots \end{aligned} \tag{14}$$

From this, we see that if we detect 1 particle in A and none in B then the output state must be projected onto $|0\rangle + \alpha e^{i\theta}|1\rangle$, which, when normalised, is precisely the truncated state given by Eq. (11).

This QST procedure will be very useful when we consider a scheme for observing superpositions between a single particle and the vacuum. It is therefore convenient to represent it more compactly as a 'black-box' as shown in Figure 2(b). This will greatly simplify our diagrams. We should point out that beam splitters have been experimentally demonstrated for atoms as well as photons [18–20] and so the QST scheme should be able to be applied to atoms. Indeed every step of the interferometry scheme that we will present is equally applicable to (bosonic) atoms as photons.

III. HADAMARD GATE

Let us now consider how we could implement a Hadamard gate in the Fock basis $\{|0\rangle, |1\rangle\}$. As we shall see, this choice of basis complicates matters. For this reason, we do not think that this is a useful basis for performing quantum

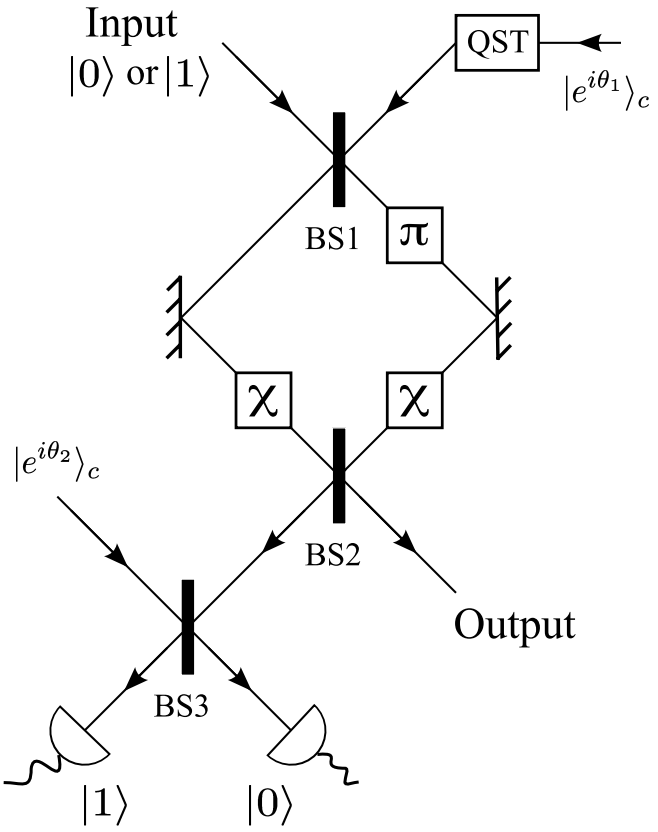

FIG. 3: The Hadamard gate scheme. This consists of three 50:50 beam splitters (BS1, BS2, and BS3), two nonlinearities (χ), a π phase shift (π) and conditional measurements made at the outputs of BS3. It also makes use of the quantum state truncation scheme shown in Figure 2. The overall transformation that this interferometer performs is given by Equations (24) and (25).

information processing protocols. However, it is interesting to consider for more fundamental reasons. One possible scheme for implementing a Hadamard gate in the Fock basis is shown in Figure 3 and consists of three 50:50 beam splitters (labelled BS1, BS2, and BS3), two ordinary mirrors, a π phase shift, and two nonlinear crystals (labelled χ). The nonlinear crystals give a phase shift to the state that depends nonlinearly on the number of particles. We take the Hamiltonian for the nonlinearity to be

$$H_\chi = \hbar\chi a^{\dagger 2}a^2 = \hbar\chi\hat{n}(\hat{n}-1), \tag{15}$$

where a is the annihilation operator corresponding to the mode on which the nonlinearity acts and $\hat{n}$ is the corresponding number operator. We will take $\chi = \pi/2$, which means that there is no phase shift if there are 0 or 1 particles in the mode, but a phase shift of π if there are 2 particles. We can confirm that this setup performs a Hadamard operation by directly calculating how it transforms the input states.

Let us begin by considering the upper part of the setup consisting of the interferometer made up of BS1 and BS2. For now we take the input state to be $|0\rangle$ (we will consider $|1\rangle$ shortly). The other input to BS1 is given by performing QST on the coherent state $|e^{i\theta_1}\rangle_c$, which has an amplitude of $\alpha = 1$. We have seen that this gives $|0\rangle + e^{i\theta_1}|1\rangle$. So the overall input state to BS1 is $|0\rangle(|0\rangle + e^{i\theta_1}|1\rangle)$, where we are ignoring the normalisation, and will use the convention that the left hand ket represents the left hand path at each point in the scheme. We can now propagate this state through the setup:

$$\begin{aligned}
|0\rangle(|0\rangle + e^{i\theta_1}|1\rangle) &\xrightarrow{BS1} |0\rangle|0\rangle + \frac{e^{i\theta_1}}{\sqrt{2}}\left(|1\rangle|0\rangle + i|0\rangle|1\rangle\right) \\
&\xrightarrow{\pi,\text{mirrors}} |0\rangle|0\rangle + \frac{e^{i\theta_1}}{\sqrt{2}}\left(i|1\rangle|0\rangle + |0\rangle|1\rangle\right) \\
&\xrightarrow{\chi} |0\rangle|0\rangle + \frac{e^{i\theta_1}}{\sqrt{2}}\left(i|1\rangle|0\rangle + |0\rangle|1\rangle\right) \\
&\xrightarrow{BS2} |0\rangle(|0\rangle + ie^{i\theta_1}|1\rangle)_{\text{out}}.
\end{aligned} \tag{16}$$

The mirrors give a $\pi/2$ phase change due to reflection and we see that the nonlinearity in this case has no effect since there is, at most, one particle on each path.

We can carry out a very similar analysis for the input $|1\rangle$. This gives

$$\begin{aligned}
|1\rangle(|0\rangle + e^{i\theta_1}|1\rangle) &\xrightarrow{BS1} \frac{1}{\sqrt{2}}\left(|0\rangle|1\rangle + i|1\rangle|0\rangle\right) + \frac{ie^{i\theta_1}}{\sqrt{2}}\left(|0\rangle|2\rangle + |2\rangle|0\rangle\right) \\
&\xrightarrow{\pi,\text{mirrors}} \frac{-1}{\sqrt{2}}\left(i|0\rangle|1\rangle + |1\rangle|0\rangle\right) - \frac{ie^{i\theta_1}}{\sqrt{2}}\left(|0\rangle|2\rangle + |2\rangle|0\rangle\right) \\
&\xrightarrow{\chi} \frac{-1}{\sqrt{2}}\left(i|0\rangle|1\rangle + |1\rangle|0\rangle\right) + \frac{ie^{i\theta_1}}{\sqrt{2}}\left(|0\rangle|2\rangle + |2\rangle|0\rangle\right) \\
&\xrightarrow{BS2} -|1\rangle(i|0\rangle + e^{i\theta_1}|1\rangle)_{\text{out}}. \qquad (17)
\end{aligned}$$

We see that these two transforms give us something close to what we want in the sense that we get two different orthogonal output states depending on the input state and these are equally weighted superpositions of $|0\rangle$ and $|1\rangle$. The problem is that these each of the output states of the second qubit are coupled to a different state of the first qubit. This wouldn't matter if we were only interested in using $|0\rangle$ or $|1\rangle$ at a time as our input. However, we want to be able to input arbitrary superpositions of these two states $c_0|0\rangle + c_1|1\rangle$, for which the output would be

$$c_0|0\rangle + c_1|1\rangle \xrightarrow{H} c_0|0\rangle(|0\rangle + ie^{i\theta_1}|1\rangle) - c_1|1\rangle(i|0\rangle + e^{i\theta_1}|1\rangle), \qquad (18)$$

and in this case, our second qubit at the output path is entangled with the first qubit at the other output from BS2. If we trace over the first qubit, we get a mixed state of $|0\rangle$ and $|1\rangle$ as our output at the second qubit, which is not what we want. To avoid this, we need to wash out this which-way information by a nonunitary operation. We do this by combining the first qubit with another state at BS3. We then detect the number of particles at the outputs and retain only the cases where we detect one particle at the left hand detector and none at the right hand one. This is reminiscent of the QST scheme described above. Let us now consider how this works for the cases of the two different input states. From (16), just before BS3 the total state is

$$|e^{i\theta_2}\rangle_c|0\rangle(|0\rangle + ie^{i\theta_1}|1\rangle)_{\text{out}} = (|0\rangle + e^{i\theta_2}|1\rangle + \cdots)|0\rangle(|0\rangle + ie^{i\theta_1}|1\rangle)_{\text{out}}. \qquad (19)$$

The first two qubits are transformed by BS3 to give:

$$\left[|0\rangle|0\rangle + \frac{1}{\sqrt{2}}e^{i\theta_2}\left(|0\rangle|1\rangle + i|1\rangle|0\rangle\right) + \cdots\right](|0\rangle + ie^{i\theta_1}|1\rangle)_{\text{out}}. \qquad (20)$$

So if we detect one particle in the left detector (1st qubit) and none in the right detector (2nd qubit), we are left with the state:

$$\frac{i}{\sqrt{2}}e^{i\theta_2}(|0\rangle + ie^{i\theta_1}|1\rangle)_{\text{out}}. \qquad (21)$$

We see that the output state is no longer correlated to another qubit, i.e. the which-way information has been washed out.

If we repeat the same analysis for the state $|1\rangle$, from (17) the input to BS3 is,

$$-|e^{i\theta_2}\rangle_c|1\rangle(i|0\rangle + e^{i\theta_1}|1\rangle)_{\text{out}}. \qquad (22)$$

If, as before, we detect one particle in the left detector and none in the right detector, we are left with the state:

$$-\frac{1}{\sqrt{2}}(i|0\rangle + e^{i\theta_1}|1\rangle)_{\text{out}}. \qquad (23)$$

Again, we have washed out the which-way information. The transformations brought about by the scheme depicted in Figure 3 can therefore be summarised as:

$$|0\rangle \longrightarrow \frac{i}{\sqrt{2}}e^{i\theta_2}(|0\rangle + ie^{i\theta_1}|1\rangle)_{\text{out}} \qquad (24)$$

$$|1\rangle \longrightarrow -\frac{1}{\sqrt{2}}(i|0\rangle + e^{i\theta_1}|1\rangle)_{\text{out}}, \qquad (25)$$

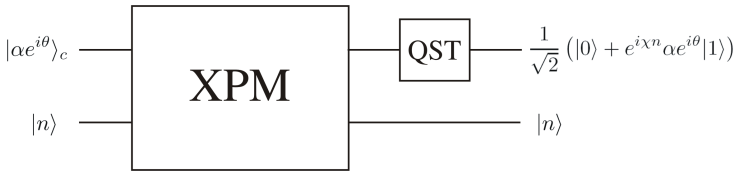

FIG. 4: An alternative way of implementing the Hadamard gate using cross phase modulation (XPM).

which is equivalent to a Hadamard gate. These transformations could be put into the form of (8) and (9) with straightforward phase shifts, but this is not necessary and we will use them in the form shown in (24) and (25).

Since the success of our scheme is conditioned on detecting particular values for some of the modes, not every run will give us the desired output. The probability of success depends on the probabilities of success for the two quantum state truncation stages as well as for the wash-out process. We have a probability of $1/(2e)$ for a quantum state truncation to succeed if it is fed with an equally weighted superposition of the vacuum and one photon state in the coherent state, i.e. for a $|e^{i\theta}\rangle_c$ state[17]. This is true for ideal photodetectors, nevertheless, even if we had photodetectors with efficiency of $\eta = 0.5$, we would still have a probability of $0.9/(2e)$ of succeeding, which is very favorable. Likewise, the success probability for the wash-out stage is obtained from the coefficient for the $|1\rangle|0\rangle$ state in the output of BS3. Since we have,

$$|e^{i\theta_2}\rangle_c|0\rangle \xrightarrow{BS3} e^{-1/2}\left(|0\rangle|0\rangle + \frac{1}{\sqrt{2}}\left(|0\rangle|1\rangle + i|1\rangle|0\rangle\right) + \cdots\right) \tag{26}$$

$$|e^{i\theta_2}\rangle_c|1\rangle \xrightarrow{BS3} e^{-1/2}\left(\frac{1}{\sqrt{2}}\left(|1\rangle|0\rangle + i|0\rangle|1\rangle\right) + \cdots\right), \tag{27}$$

then, we get a probability of $1/(2e)$ of success for ideal photodetectors. Consequently, the probability of success for the full apparatus is $(1/(2e))^3 = 6.2 \times 10^{-3}$, i.e. the scheme will success in approximately 3 out of 500 attempts. We can significantly increase this probability with a little extra effort. For instance, we can double the success probability in the QST stages if we do not disregard the output state when we detect 1 particle in B and none in A in Figure 2(a) and instead we subject it to a phase shift of π.

The scheme we have discussed for a Hadamard gate in the Fock basis is just one possible realisation and there may be simpler schemes. One example is to use a cross-nonlinearity that depends on the number of particles in different modes, as depicted in Figure 4. The idea behind this scheme is that the relations in Eqs. (8) and (9) could be realised by means of a controlled phase shift applied to a truncated state obtained via the QST scheme. This controlled phase should apply no phase shift to a truncated state if a $|0\rangle$ is received as the control input qubit and should apply a π phase if a $|1\rangle$ state is received instead. The scheme in Figure 4 does exactly that by using a cross phase modulation effect between the Fock state and the coherent state and finally, truncating the later. The Hamiltonian of the cross phase modulation is,

$$H = \hbar\chi a^\dagger a b^\dagger b, \tag{28}$$

where a and b are the anihilation operators for the two different modes and χ is a coefficient related to the strength of the nonlinearity. If we take $\chi = \pi$, the scheme shown in Figure 4 would give the following transformations (for $\alpha = 1$),

$$|0\rangle|e^{i\theta}\rangle_c \xrightarrow{H} \frac{1}{\sqrt{2}}|0\rangle\left(|0\rangle + e^{i\theta}|1\rangle\right) \tag{29}$$

$$|1\rangle|e^{i\theta}\rangle_c \xrightarrow{H} \frac{1}{\sqrt{2}}|1\rangle\left(|0\rangle - e^{i\theta}|1\rangle\right). \tag{30}$$

We could then wash out the which-way information contained in the first qubit using the same procedure as described above. This gives us an alternative way of constructing the Hadamard gate, which seems simpler at least schematically. For now, however, we will concentrate on the first scheme as shown in Figure 3. This is because we would like our scheme to be applicable to (bosonic) atoms as well as photons and it is not clear how the cross nonlinearity could be easily achieved for atoms. We should point out that our scheme is restricted to bosons because it relies on having coherent states of the particles, which are not physical for fermions. We also make use of the property that two bosons from different arms of a beam splitter bunch in the Hadamard transform (17).

IV. INTERFEROMETER

The signature of a superposition of a particle and the vacuum (as in states (24) and (25)), is interference between the two components. We could observe this interference by combining two Hadamard gates with a phase shift, ϕ, between them to create a simple interferometer as shown in Figure 5(a). If we find that the probability of detecting the final state in Figure 5(a) depends on the value of ϕ, then this will confirm the coherence of the superposition of $|0\rangle$ and $|1\rangle$ after the first Hadamard.

The problem with this 'simple' interferometer is that it hides a lot of complexity: each Hadamard is implemented by the scheme shown in Figure 3 and the whole scheme involves two quantum state truncations and two procedures to wash out the which-way information. So it is quite complicated schematically, to say nothing of how it might be experimentally realised. We can, however, simplify things considerably if we consider only a particular input to our interferometer, let's say the vacuum, $|0\rangle$. In this case, the first Hadamard gate in Figure 5(a) creates a coherent superposition of one particle and the vacuum. However, the same thing could be achieved by taking advantage of the QST scheme again, since it can truncate a coherent state to leave us only with a superposition of one particle and the vacuum. Consequently, the input state and first Hadamard gate can be replaced by a coherent state and the QST gate, respectively, as it is shown in Figure 5(b). This simpler scheme should be enough to observe interference fringes between the $|0\rangle$ and $|1\rangle$ states and so confirm their superposition. Let us now consider how this works.

After the input state, $|e^{i\theta}\rangle_c$, has been truncated and had a phase shift, ϕ, applied to it (i.e. the first two steps in Figure 5(b)), we end up with the state,

$$\frac{1}{\sqrt{2}}\left(|0\rangle + e^{i(\theta+\phi)}|1\rangle\right). \tag{31}$$

This is then passed through a Hadamard gate using the scheme shown in Figure 3. We have seen that this gate performs the transformations given by Eq. (24) and Eq. (25) and so the final state is

$$\begin{aligned}\frac{1}{\sqrt{2}}\left(|0\rangle + e^{i(\theta+\phi)}|1\rangle\right) \xrightarrow{H} & \frac{i}{2}e^{i\theta_2}\left(|0\rangle + ie^{i\theta_1}|1\rangle\right) - \frac{1}{2}e^{i(\theta+\phi)}\left(i|0\rangle + e^{i\theta_1}|1\rangle\right) \\ &= ie^{i\theta_2}\left(\frac{1-e^{i(\theta+\phi-\theta_2)}}{2}\right)|0\rangle - e^{i\theta_2}e^{i\theta_1}\left(\frac{1+e^{i(\theta+\phi-\theta_2)}}{2}\right)|1\rangle \\ &= e^{i\theta_2}e^{i\frac{\theta+\phi-\theta_2}{2}}\left[\left(\frac{e^{i\frac{\theta+\phi-\theta_2}{2}} - e^{-i\frac{\theta+\phi-\theta_2}{2}}}{2i}\right)|0\rangle - e^{i\theta_1}\left(\frac{e^{i\frac{\theta+\phi-\theta_2}{2}} + e^{-i\frac{\theta+\phi-\theta_2}{2}}}{2}\right)|1\rangle\right],\end{aligned} \tag{32}$$

where we can neglect the global phase factored out in the last step since overall phases in the state vector are unobservable and have no physical consequences. The final state can therefore be written as

$$\sin\left(\frac{\phi+\theta-\theta_2}{2}\right)|0\rangle - e^{i\theta_1}\cos\left(\frac{\phi+\theta-\theta_2}{2}\right)|1\rangle. \tag{33}$$

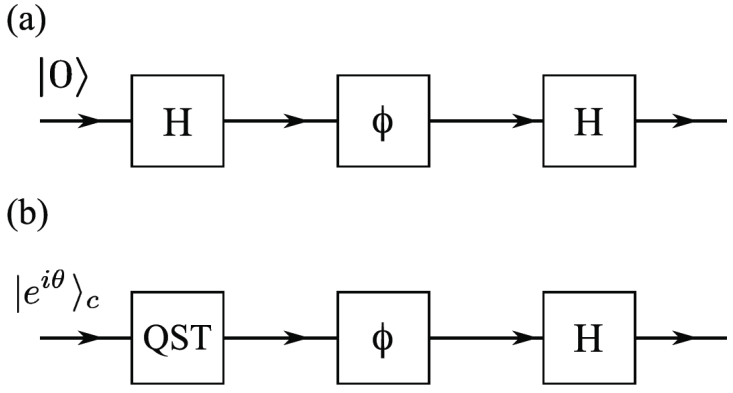

FIG. 5: (a) The general Hadamard interferometery scheme. An input state in the basis $\{|0\rangle, |1\rangle\}$ is transformed with a Hadamard gate, a phase shift, ϕ, and then a second Hadamard gate. (b) The scheme can be simplified if we are only interested in a specific case that can demonstate the superposition of a single particle and the vacuum. In this case, quantum state truncation is used to give the superposition state (similar to the output of the first Hadarmard in (a)). This state then undergoes a phase shift and a Hadamard transformation.

This state depends on all four phases ϕ, θ, θ_1, and θ_2. However, the magnitudes of the coefficients of $|0\rangle$ and $|1\rangle$ depend only on $\phi+\theta-\theta_2$, i.e. they are independent of θ_1. This is what we might expect since the the coefficients depend on the relative phase of the two paths "inside" the interferometer, i.e. the input to the Hadamard $(\theta+\phi)$ and the reference state input to BS3 (θ_2).

From (33), the probabilities of measuring one particle and none at the output of the interferometer are respectively,

$$P_1 = \cos^2\left(\frac{\phi+\theta-\theta_2}{2}\right), \tag{34}$$

$$P_0 = \sin^2\left(\frac{\phi+\theta-\theta_2}{2}\right). \tag{35}$$

This looks promising as we have interference fringes at the output that depend on the applied phase ϕ. However, the fringes also depend on θ and θ_2, which presents a problem. To see interference fringes, we need to repeat the experiment many times for each value of ϕ in order to find the values of P_0 and P_1. However the phases of coherent states that are independently produced are not fixed and vary randomly from run to run. This means that on the ensemble average we need to average over all phases θ and θ_2 and, consequently, the interference fringes will wash out.

We can overcome this problem by fixing their *relative* value, i.e. $\theta-\theta_2$ by creating them from the same source. In Figure 6, we show how this could be achieved by introducing another beam splitter (BS4) to create the states $|e^{i\theta}\rangle_c$ and $|e^{i\theta_2}\rangle_c$ so that their phase is the same on every run, i.e. $\theta-\theta_2=0$. In this case, the output probabilities are:

$$P_1 = \cos^2\left(\frac{\phi}{2}\right), \tag{36}$$

$$P_0 = \sin^2\left(\frac{\phi}{2}\right). \tag{37}$$

This means that inference fringes should be able to be built up over an ensemble of runs since the position of the fringes now depends only on the controllable parameter, ϕ. This suggests that we should be able to use this scheme to observe the interference of different Fock states.

V. MIXED STATES

So far it seems that, in order to observe a superposition of the form of (1), we need to start with a superposition in the Fock basis (i.e. a coherent state). This seems like a circular argument. However, in this section, we show that we do not need superpositions in the Fock basis as our initial states. In fact, we can use mixed state inputs.

The mixed state,

$$\rho = e^{-|\alpha|^2}\sum_{n=0}^{\infty}\frac{|\alpha|^{2n}}{n!}|n\rangle\langle n| \tag{38}$$

is formally equivalent to a coherent state with amplitude $|\alpha|$ averaged over all phases, i.e.

$$\rho = \frac{1}{2\pi}\int_0^{2\pi}||\alpha|e^{i\theta}\rangle\langle|\alpha|e^{i\theta}|\,d\theta, \tag{39}$$

since

$$\begin{aligned}\frac{1}{2\pi}\int_0^{2\pi}||\alpha|e^{i\theta}\rangle\langle|\alpha|e^{i\theta}|\,d\theta &= \frac{1}{2\pi}\int_0^{2\pi}e^{-|\alpha|^2/2}\sum_{n=0}^{\infty}\frac{(|\alpha|e^{i\theta})^n}{\sqrt{n!}}|n\rangle e^{-|\alpha|^2/2}\sum_{m=0}^{\infty}\frac{(|\alpha|e^{-i\theta})^m}{\sqrt{m!}}\langle m|\,d\theta \\ &= e^{-|\alpha|^2}\sum_{n=0}^{\infty}\sum_{m=0}^{\infty}\frac{|\alpha|^{n+m}}{\sqrt{n!}\sqrt{m!}}\left(\frac{1}{2\pi}\int_0^{2\pi}e^{i\theta(n-m)}\,d\theta\right)|n\rangle\langle m| \\ &= e^{-|\alpha|^2}\sum_{n=0}^{\infty}\frac{|\alpha|^{2n}}{n!}|n\rangle\langle n|, \end{aligned} \tag{40}$$

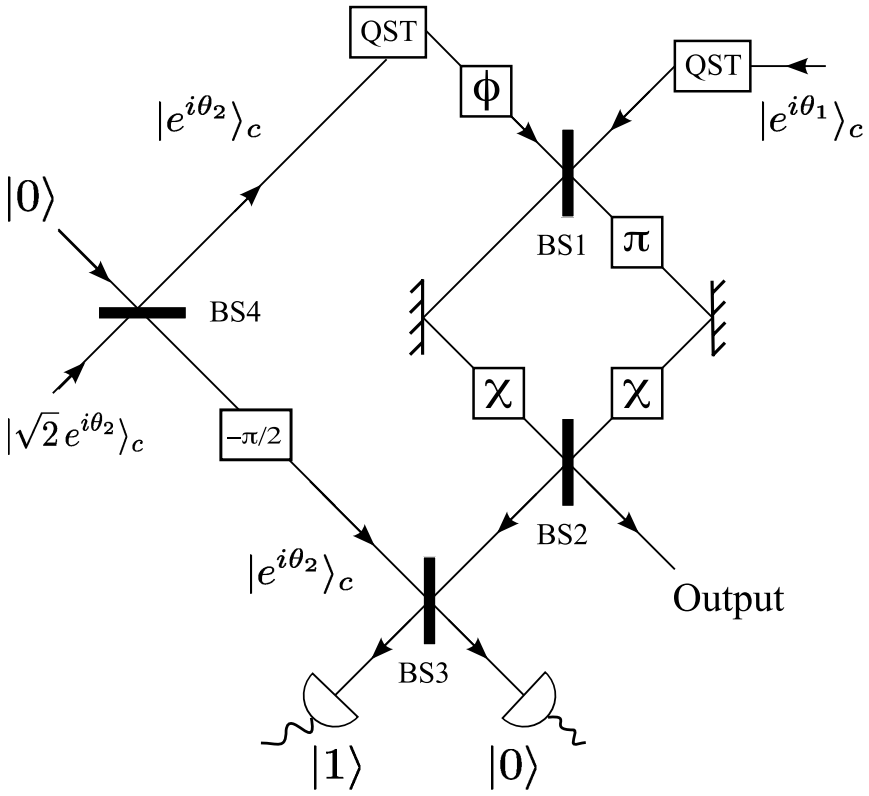

FIG. 6: The full scheme for demonstrating interference between a single particle and the vacuum as given in Figure 6(b). Importantly, as discussed in the text, the phase of the input to the QST scheme on the left and the input to the which-way wash-out scheme at BS3 have their phases fixed. This is achieved by creating them from a common source at BS4.

where in the last step we used the fact that the integral in parentheses evaluates to δ_{nm}. This means that, if $\rho_{\rm M} = \rho_1 \otimes \rho_2 \otimes \ldots$ is the input density matrix to our full interferometer shown in Figure 6 with mixed states

$$\rho_1 \;=\; e^{-2}\sum_{n=0}^{\infty}\frac{2^n}{n!}|n\rangle\langle n| \tag{41}$$

$$\rho_2 \;=\; e^{-1}\sum_{n=0}^{\infty}\frac{1}{n!}|n\rangle\langle n|, \tag{42}$$

instead of coherent states, and $U_{\rm I}$ represents the evolution operator for this interferometer, then the output density matrix would be

$$\rho_{\rm M} \xrightarrow{U_{\rm I}} U_{\rm I}\rho_{\rm M}U_{\rm I}^{\dagger} = \frac{1}{(2\pi)^2}\int_0^{2\pi}\int_0^{2\pi} d\theta_1 d\theta_2 U_{\rm I}\rho_{\rm C}U_{\rm I}^{\dagger}, \tag{43}$$

where $\rho_{\rm C}$ is the input density matrix using the coherent states $|\sqrt{2}e^{i\theta_2}\rangle_c$ and $|e^{i\theta_1}\rangle_c$. Therefore, the output is just what we calculated earlier for these inputs , but averaged over all phases θ_1 and θ_2 . From (33), we see that we get the output

$$\rho = \sin^2\left(\frac{\phi}{2}\right)|0\rangle\langle 0| + \cos^2\left(\frac{\phi}{2}\right)|1\rangle\langle 1|, \tag{44}$$

where we have used the fact that relative values of θ and θ_2 are fixed, i.e. $\theta - \theta_2 = 0$ and we have averaged over θ_1 and θ_2. The output state is therefore a mixture of a single particle and the vacuum. However, the interesting thing is that the probabilities of detecting one or no particles at the output are not affected, i.e. they are just the same as those given in (36) and (37) even though our inputs are mixed states. Does this result still mean that we have a superposition of a single particle and the vacuum inside the interferometer? In itself, no. But we can argue that this interpretation is consistent with our results if we think more carefully about the state where the phase, ϕ, is applied.

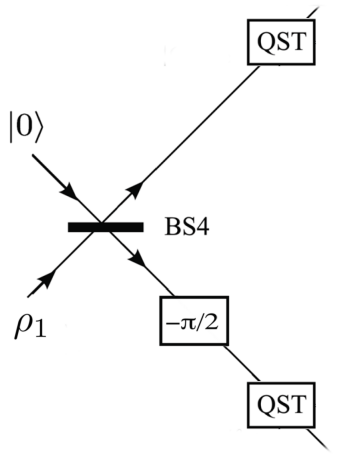

FIG. 7: Mixed state ρ_1 as input to the interferometer and QST stage addition.

In order to do this, it is convenient to slightly modify the scheme shown in Figure 6 by adding a QST step after the $-\pi/2$ phase shift on the lower output from BS4. This modification is shown in Figure 7. It is easy to see that this doesn't affect the final output from the interferometer because it just throws away all cases where there were two or more particles on that path. However, the post-selection procedure at BS3 achieved the same effect.

If we consider the particular mixed state ρ_1 given by Eq. (41) as the input to the 50:50 beam splitter BS4 in Figure 7, then the output state after the QST on each path can be shown to be

$$\rho_1 \longrightarrow \frac{1}{4}\left(|0,0\rangle\langle 0,0| + |1,1\rangle\langle 1,1| + |0,1\rangle\langle 0,1| + |1,0\rangle\langle 1,0| + |0,1\rangle\langle 1,0| + |1,0\rangle\langle 0,1|\right). \tag{45}$$

We can see that this state is not entangled by taking the partial transpose and checking that there are no negative eigenvalues [21]. This means that the upper path after the QST operation is not entangled with the lower (reference) path after the QST operation. This is important because it means that when the phase, ϕ, is applied to the upper path, it should depend only on the state on that path (i.e. it is completely independent of the reference path). However, we know that the output from the full scheme (44) depends coherently on the phase that is applied. This suggests that the state on the path where ϕ is applied is a superposition of number states. If we had a number state or a mixture of number states at that point then the phase would not alter the state, i.e.

$$\rho = \sum_n P_n |n\rangle\langle n| \xrightarrow{\phi} \sum_n P_n e^{in\phi} |n\rangle\langle n| e^{-in\phi} = \rho, \tag{46}$$

where P_n are general probabilities. So what is going on? The total state (45) is mixed and yet the output from the scheme shown in Figure 6 suggests that the upper path is in a superposition of a single particle and the vacuum. The answer is that the upper path is in a mixed state *on average* and we need to think about what happens run by run.

One way of consistently interpreting these conclusions is that, on a given run, the output state of BS3 after the two QST operations is

$$\frac{1}{2}\left(|0\rangle + e^{i\theta}|1\rangle\right)\left(|0\rangle + e^{i\theta}|1\rangle\right), \tag{47}$$

where θ is a random phase and the left and right qubits respectively represent the upper and lower paths. On a single shot, we have a superposition of a single particle and the vacuum where the phase, ϕ, acts on the upper path. However, averaging over all phases gives us the mixed state (45). Normally, these two interpretations would be indistinguishable since an interference pattern needs to be built up over many detections and the fringes would wash out. In the present case, however, we have arranged things so that the lower path *keeps track* of the random phase on each run. We can see this from (47) where the lower state has a record of the same random phase that appears in the upper path. This allows us to reconstruct the interference pattern indicating that we had a superposition of different Fock states inside the interferometer. This emphasises the importance of the lower (reference) path. Without it no interference pattern would be seen.

VI. CONCLUSIONS

We have proposed an experimentally feasible scheme that should enable us to see interference between a single particle and the vacuum. This scheme is applicable to both optical and atomic mixed states, which means we don't need to assume superpositions of different Fock states in order for it to work. It would be interesting to see if similar schemes could be realised for a broader range of physical systems or if there are fundamental limitations that prevent this.

The output from the interferometer shown in Figure 6 is a mixed state and so it is important to note that our scheme does not *prepare* superpositions of different Fock states that could, for example, then be used in other protocols. However, the probability of detecting one or no particles at the output depends coherently on a controllable external phase. This is consistent with the interpretation that there was a coherent superposition inside the interferometer at the point at which the phase, ϕ, was applied.

What we have presented is really a 'proof of principle' that evidence consistent with non-number-conserving superpositions could be observed in low energy non-relativistic experiments. There may very well be simpler schemes for doing this. It certainly is a fascinating idea and it will be interesting to see how far its applicability can be extended to other superpositions that violate superselection rules.

VII. ACKNOWLEDGEMENTS

This work was supported by Consejo Nacional de Ciencia y Teconologia(CONACyT, Mexico), Secretaria de Educacion Publica(SEP, Mexico) and the United Kingdom EPSRC through an Advanced Research Fellowship GR/S99297/01, an RCUK Fellowship, and the EuroQUASAR programme EP/G028427/1.

---

[1] G. C. Wick, A. S. Wightman, and E. P. Wigner, Phys. Rev. **88**, 101 (1952).
[2] Y. Aharonov and L. Susskind, Phys. Rev. **155**, 1428 (1967).
[3] R. Mirman, Phys. Rev. **186**, 1380 (1969).
[4] A. Kitaev, D. Mayers, and J. Preskill, Phys. Rev. A **69**, 052326 (2004).
[5] S. D. Bartlett, A. C. Doherty, R. W. Spekkens, and H. M. Wiseman, Phys. Rev. A **73**, 022311 (2006).
[6] M. R. Dowling, S. D. Bartlett, T. Rudolph, and R. W. Spekkens, Phys. Rev. A **74**, 052113 (2006).
[7] M. O. Terra Cunha, J. A. Dunningham, and V. Vedral, Proc. Roy. Soc. A **463**, 2277 (2007).
[8] T. Paterek, P. Kurzyński, D. Oi and D. Kaszlikowski, arXiv:quant-ph/1004.5184.
[9] S. M. Tan, D. F. Walls, and M. J. Collett, Phys. Rev. Lett. **66**, 252 (1991).
[10] L. Hardy, Phys. Rev. Lett. **73**, 2279 (1994).
[11] E. Santos, Phys. Rev. Lett. **68**, 894 (1992).
[12] S. M. Tan, D. F. Walls, and M. J. Collett, Phys. Rev. Lett. **68**, 895 (1992).
[13] G. Björk, P. Jonsson, and L. L. Sánchez-Soto, Phys. Rev. A **64**, 042106 (2001).
[14] J. A. Dunningham and V. Vedral, Phys. Rev. Lett. **99**, 180404 (2007).
[15] J. A. Dunningham, V. Palge and V. Vedral, Phys. Rev. A **80**, 044302 (2009).
[16] Pieter Kok, arXiv:quant-ph/0705.4193.
[17] D. T. Pegg, L. S. Phillips, and S. M. Barnett, Phys. Rev. Lett. **81**, 1604 (1998).
[18] O. Carnal and J. Mlynek, Phys. Rev. Lett **66**, 2689 (1991).
[19] D. Keith, C. Ekstrom, Q. Turchette, and D. Pritchard, Phys. Rev. Lett **66**, 2693 (1991).
[20] F. Riehle, T. Kisters, A. Witte, J. Helmcke, and C. Borde, Phys. Rev. Lett. **67**, 177 (1991).
[21] M. Horodecki, P. Horodecki, and R. Horodecki, Phys. Lett. A **223**, 1 (1996).